In-beam performance of neutron irradiated MIMOSIS-1 CMOS Monolithic Active Pixel Sensors

Published by IOP Publishing for Sissa Medialab

Received: *May 15, 2025*
Accepted: *July 9, 2025*
Published: *August 12, 2025*

20th Anniversary Trento Workshop on Advanced Silicon Radiation Detectors
Trento, Italy
4–6 February 2025

In-beam performance of neutron irradiated MIMOSIS-1 CMOS Monolithic Active Pixel Sensors

Hasan Darwish[a,c,*] **Ali-Murteza Altingun**[c] **Julio Andary**[a] **Benedict Arnoldi-Meadows**[a] **Jerome Baudot**[c] **Gregory Bertolone**[c] **Auguste Besson**[c] **Norbert Bialas**[a] **Christopher Braun**[a] **Roma Bugiel**[c] **Gilles Claus**[c] **Claude Colledani**[c] **Michael Deveaux**[a,b] **Andrei Dorokhov**[c] **Guy Dozière**[c] **Ziad El Bitar**[c] **Ingo Fröhlich**[a,b] **Mathieu Goffe**[c] **Benedikt Gutsche**[a] **Abdelkader Himmi**[c] **Christine Hu-Guo**[c] **Kimmo Jaaskelainen**[c] **Oliver Keller**[f] **Michal Koziel**[a] **Franz Matejcek**[a] **Jan Michel**[a] **Frederic Morel**[c] **Christian Müntz**[a] **Hung Pham**[c] **Christian Joachim Schmidt**[b] **Stefan Schreiber**[a] **Marvin Schulz**[a] **Matthieu Specht**[c] **Joachim Stroth**[a,b,d] **Eva-dhidho Taka**[a] **Isabelle Valin**[c] **Yüe Zhao**[c] **and Marc Winter**[e]

[a] *Institut für Kernphysik, Goethe-Universität Frankfurt, Max-von-Laue-Straße 1, 60438 Frankfurt, Germany*
[b] *GSI Helmholtzzentrum für Schwerionenforschung GmbH, Planckstraße 1, 64291 Darmstadt, Germany*
[c] *Université de Strasbourg, CNRS, IPHC UMR 7178, 67037 Strasbourg, France*
[d] *Helmholtz Forschungsakademie Hessen für FAIR, Max-von-Laue-Straße 12, 60438 Frankfurt, Germany*
[e] *Université Paris-Saclay, CNRS/IN2P3, IJCLab, 91405 Orsay, France*
[f] *Facility for Antiproton and Ion Research GmbH, Planckstraße 1, 64291 Darmstadt, Germany*

E-mail: h.darwish@gsi.de

Abstract: MIMOSIS is the CMOS Monolithic Active Pixel Sensor designed for the Micro Vertex Detector (MVD) of the Compressed Baryonic Matter (CBM) experiment currently under development at FAIR. The sensors have to combine a spatial and a time resolution of 5 µm and 5 µs, handle a peak hit rate of ~ 80 MHz/cm^2, and to withstand Total Ionizing radiation Doses (TID) of ~ 5 MRad and Non-Ionizing Energy Loss (NIEL) fluences of ~ 7×10^{13} n_{eq}/cm^2 before being replaced. Prior to their use in the experiment, the sensors undergo lab and in-beam tests, to qualify their performance in charged particles detection. In this work we present the sensor design and concept, a summary of its requirements as a candidate for the CBM-MVD, followed by the performance results of the first full-size prototype, MIMOSIS-1, from in-beam tests done at DESY and CERN, after being irradiated to different TID and NIEL fluences.

Keywords: Particle tracking detectors (Solid-state detectors); Pixelated detectors and associated VLSI electronics; Radiation-hard detectors; Si microstrip and pad detectors

*Corresponding author.

https://doi.org/10.1088/1748-0221/20/08/C08009

Contents

1 Introduction

The MIMOSIS CMOS Monolithic Active Pixel Sensor is designed to equip the Micro Vertex Detector (MVD) [1] of the Compressed Baryonic Matter (CBM) experiment [2] currently under development at FAIR facility in Darmstadt, Germany. CBM is a future fixed-target heavy-ion experiment designed to explore the QCD phase diagram in the region of high baryon densities [2]. This will be achieved by probing hot and highly compressed baryonic matter with rare multi-strange and charm particles, produced in heavy ion collisions of Au+Au (and p+A) with beam energies of up to 10 *A*GeV (and 28 GeV). The targeted collision rates amount to 100 kHz (and 10 MHz for p+A) if the MVD is operated in the experiment. Up to two orders of magnitude higher rates are possible at CBM for observables not requiring the MVD. The MVD optional fast removal was considered in the design process when the experiment physics cases do not mandate its use.

The MVD is designed for the aim of separating primary and secondary vertices of weakly decaying particles, and to contribute in the low momentum particles tracking with other subdetectors. The CBM physics goals and running conditions drive towards very challenging requirements on the MVD. It is composed of four planar stations that are placed in the target vacuum at distances of 5–20 cm downstream the fixed target. Being close to the target and at a 5.4 mm distance from the beam axis, it will be exposed to a dense flux of charged particles coming from the collision, as well as possible target fragments or beam halo ions.

The sensors equipping the MVD will have to handle high hit rates reaching an average of 20 MHz/cm^2, with a maximum of 80 MHz/cm^2 in the case of beam intensity spikes. Due to the fixed target geometry, on-sensor radiation gradients reach one order of magnitude. The sensors should withstand Total Ionizing radiation Doses (TID) of $\sim$ 5 MRad and Non-Ionizing Energy Loss (NIEL) fluences of $\sim 7 \times 10^{13}$ n_{eq}/cm^2 before being replaced after one year of operation. Moreover, an LET tolerance of up to $\gtrsim$ 35 MeV cm^2/mg is required. A spatial resolution of $\sim$ 5 µm, and a continuous global shutter readout with a time binning of 5 µs has to be combined with an ultra low material budget of 50 µm silicon (0.05% X_0).

To respond to these requirements, a joint R&D project of IPHC-Strasbourg, IKF-Frankfurt and GSI, has been initiated to develop a novel CMOS Monolithic Active Pixel Sensor named MIMOSIS. The related R&D project is divided into 4 prototyping steps, MIMOSIS-0/1/2/3, each aiming to overcome

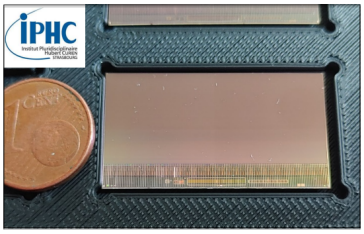

Figure 1. Photograph of the MIMOSIS-1 sensor.

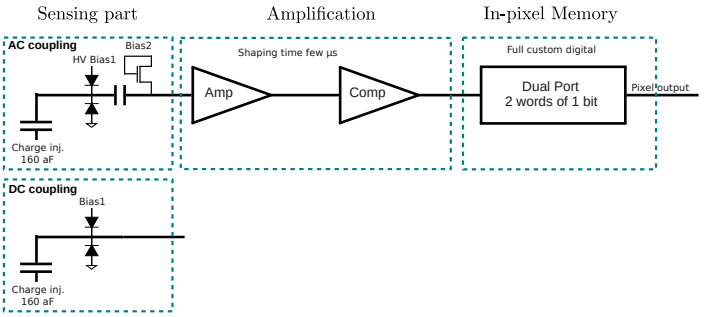

Figure 2. Block diagram of the AC (top) and DC (bottom) coupled pixels.

possible weaknesses of the previous prototype and to add features in an iterative way. In previous works we discussed results from SEE tests with MIMOSIS-1 [3], its response to particle beams with different dE/dx [4], and studies on the tolerance of MIMOSIS-1 to ionizing radiation [5]. In this work we complement these studies by reporting on the tolerance of the MIMOSIS-1 sensors to non-ionizing radiation.

2 Sensor design

MIMOSIS-1, shown in figure 1, relies on an industrial 180 nm CMOS imaging process and integrates both, the sensing elements and the analog and digital front-end electronics on the same substrate. The sensor features 1024 × 504 pixels with ~27 × 30 µm^2 pitch. Two different analog front-ends were tested: the DC-coupled pixels, as known from ALPIDE [6], allowing for a substrate bias of up to 6 V; and AC-coupled pixels suited to further extend the depletion region by the means of an additional top-bias (HV) of up to 20 V. The structures of the two pixel types are shown in the block diagram of figure 2. In the AC pixel, the sensing node and the preamplifier were galvanically decoupled by a capacitor to respect the 1.8 V voltage limit of the input transistor of the amplifier. While the depletion voltage (HV-Bias1 in the figure) is directly injected from an external power supply, the voltage denoted as Bias2 is generated by an internal DAC. The diode-connected NMOS transistor used for injecting this voltage acts as forward biased diode. Moreover, its source implantation together with the P-WELL bulk realizes a reverse biased PN-junction. This creates a diode based voltage divider similar to the sensing element, which sets the dark potential at the input of the amplifier close to V_{bias2} but has too high impedance to deteriorate the fast particle signals.

MIMOSIS-1 was realized with three different doping profiles: the "standard" pixel as produced and used already with the ALPIDE sensor [6], and the "n-gap" and "p-stop" pixels. The latter two pixels feature a low-dose n-type layer along the pixel, with a gap on the edges for the "n-gap", or an extra deep p-well for the "p-stop" [7, 8]. Both pixels were designed for the aim of fully depleting the epitaxial layer, to result in higher radiation hardness. Cross section sketches of the three pixel types are shown in figure 3.

Two different kinds of pre-amplifiers, differing slightly by transistor dimensions, were tested but no significant difference in their performance was observed. Therefore this work will restrict itself to the baseline design chosen for the consecutive prototypes and report about the test results of 6 pixel flavors ("standard", "n-gap" and "p-stop", each as DC- or AC-coupled) as obtained from laboratory tests and beam tests performed at DESY and the CERN-SPS.

2025 JINST 20 C08009

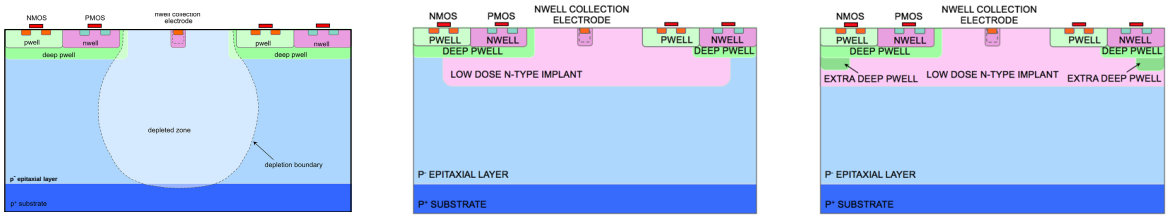

(a) Standard (b) “n-gap” (c) “p-stop”

Figure 3. Cross-sections of three pixel options differing in their epitaxial layer doping profiles, used in MIMOSIS-1. Reproduced from [7]. CC BY 4.0. Reproduced from [8].

3 Experimental setup

Different sensors under test were irradiated separately with ionizing and non-ionizing radiation and their performance was compared to the one of the non-irradiated ones. This separation was motivated by the aim of studying the effect of each type of radiation on the sensors, supported by theory and experience from previous sensors that indicate different radiation damage effects caused by the two different types. For the ionizing radiation, chips were irradiated at room temperature with a 60 kV X-ray generator with tungsten anode and vanadium filter, at the Karlsruhe Institute of Technology (KIT) in Germany. For non-ionizing radiation, chips were irradiated with ∼1 MeV reactor neutrons at the TRIGA reactor facility in Ljubljana, Slovenia. In both times, the dosimetry was carried out by the on-site operators. Its uncertainty is considered to amount to about 10%. In this work we discuss results of sensors tested with beams after being irradiated with fluences of 3×10^{13} n_{eq}/cm^2, 10^{14} n_{eq}/cm^2 and 3×10^{14} n_{eq}/cm^2, and a combined irradiation dose of 5 MRad + 10^{14} n_{eq}/cm^2. The chips were stored and tested at room temperature.

The beam tests were done using a telescope composed of 6 MIMOSIS-1 chips that were mounted on PCBs. The PCBs were placed in aluminum holders with beam openings that were covered by black tape. The aluminum holders were screwed on a liquid cooled support plate. Aiming for a sensor operation under a stabilized room temperature, a 15 °C coolant temperature was chosen. The distance between the planes was minimized as mechanically possible, reaching 1.5 cm. The two outer pairs of sensors were considered as reference (REF) planes. They were realized with 60 µm thick MIMOSIS-1 sensors with the “standard” process operating at 120 mV pixel discriminator threshold with -1 V substrate bias (BB), and 10 V top-bias (HV) for the AC-coupled pixels. The remaining two planes in the middle were operated as Devices Under Test (DUT).

The beam test data was stored and analyzed afterwards with the TAF data analysis package [9]. In the analysis, one hit in each reference plane was demanded to reconstruct a reference track. Hits on the DUT were matched to these tracks and processed in the analysis if they were found within a spatial cut distance amounting for 100 µm (∼3 × pixel pitch). The sensors were synchronized and operating with 5 µs long frames (time bins), but 5 consecutive frames were merged into one event to compensate in an easy way the effects of signal time walk [10]. The measurements were conducted with a 5 GeV/c electron beam at DESY, and a 120 GeV/c pion beam at CERN-SPS. The spatial resolution was extracted from the residuals by subtracting the telescope resolution term which was estimated by the Telescope Optimizer online tool [11] accounting for the specific beam energy and telescope geometry.

2025 JINST 20 C08009

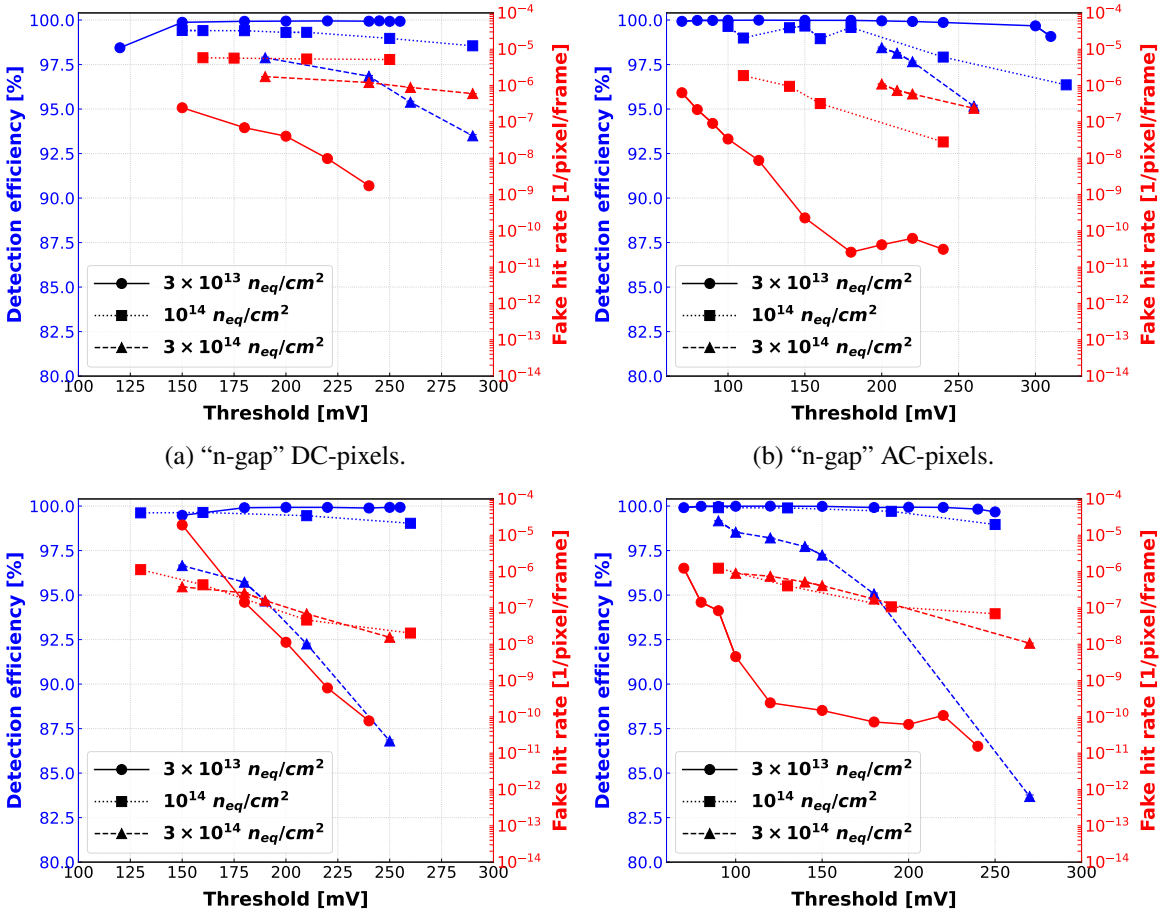

(a) "n-gap" DC-pixels.

(b) "n-gap" AC-pixels.

(c) "p-stop" DC-pixels.

(d) "p-stop" AC-pixels.

Figure 4. Detection efficiency (in blue) and fake hit rate (in red) as function of the discriminator threshold. The different sub-figures correspond to different pixel types. The different neutron irradiation levels are shown in different line styles. The measurements in this figure and the following ones (unless mentioned otherwise) were conducted with -3 V BB, and 10 V HV for the AC pixels.

4 Results

All six pixel flavors, each being irradiated with different doses reaching $\sim 3 \times 10^{14}$ n_{eq}/cm^2, were tested for detection efficiency, fake hit rate, cluster multiplicity and spatial resolution. The detection efficiency (in blue) and fake hit rate (in red), as function of the in-pixel discriminator threshold and fluence, are shown for the "n-gap" process in figure 4(a) (DC-pixels) and figure 4(b) (AC-pixels), as well as for the "p-stop" process in figure 4(c) (DC-pixels) and figure 4(d) (AC-pixels). The detection efficiency, for the four pixel types, is within an excellent range (above 99%), for the two lower fluence, with a mild drop for the maximum fluence tested. Still, a detection efficiency above 98% is observed for a fluence of $\sim 3 \times 10^{14}$ n_{eq}/cm^2, which provides a comfortable margin with respect to the requirements.

The detection efficiency and fake hit rate for all pixels and after irradiation with 10^{14} n_{eq}/cm^2 are compared in figure 5. As expected, the "n-gap" and "p-stop" pixels outperform the standard pixel, which however maintains reasonable performances at low thresholds. This could be even improved if a 20 V HV was applied during the tests. For the fake hit rate (in red), the three different pixel types,

2025 JINST 20 C08009

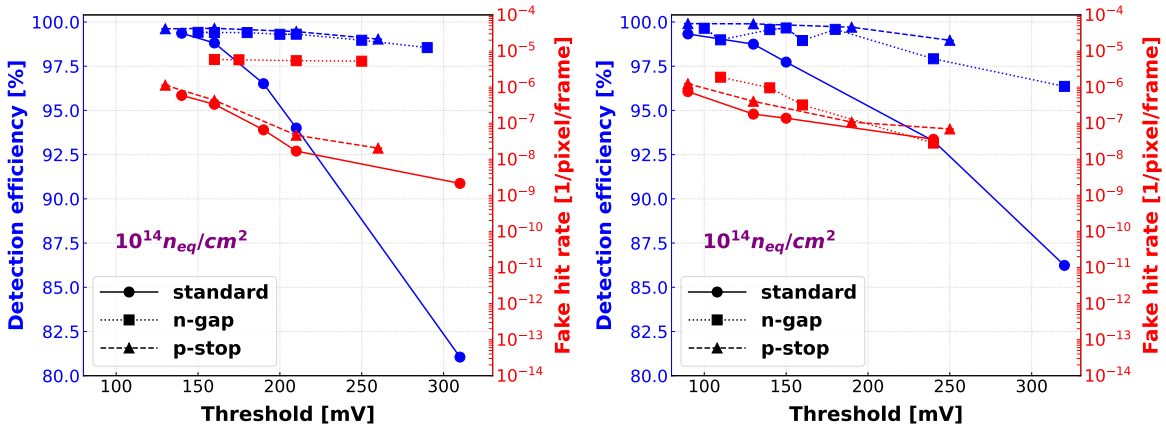

(a) DC-pixels. (b) AC-pixels.

Figure 5. Detection efficiency (blue) and fake hit rate (red) as function of threshold for DC-pixels (left) and AC-pixels (right). The three different pixel types (standard, "n-gap" and "p-stop") are shown in different line styles.

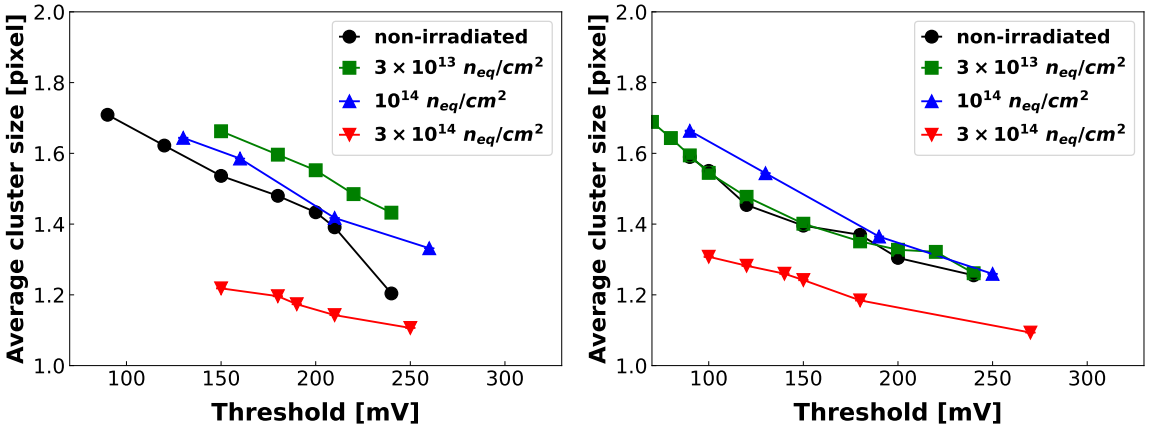

(a) DC-pixels. (b) AC-pixels.

Figure 6. Average cluster size as function of the threshold of different "p-stop" pixels sensors for DC-pixels (left) and AC-pixels (right). The different irradiation levels are shown in different colors.

also whether DC or AC, showed a good performance that fits within the requirements, being $\sim 10^{-5}$ hits per pixel per frame, and below. The bulk damage created by non-ionizing radiation is known to reduce the lifetime of the signal electrons and thus to reduce the charge collection efficiency. This may reduce the cluster multiplicity (fired pixels/particle hit) as some pixels do not reach the threshold. This hypothesis was tested and the average cluster size for the different pixel options was compared for the different previously mentioned neutron irradiation fluences, see figure 6. The expected effect is indeed observed for the highest fluence applied while no clear trend is visible for the lower ones.

The spatial resolution as function of threshold, fluence and pixel type is shown in figure 7. Most of the data points in the 4 plots that corresponds to the 4 pixel types ("n-gap" or "p-stop", whether DC or AC) indicate values between 5 and 6 µm, which is considered acceptable for the MVD. The effect of irradiation on the spatial resolution remains below $\sim$ 0.5 µm. The effect of an additional

2025 JINST 20 C08009

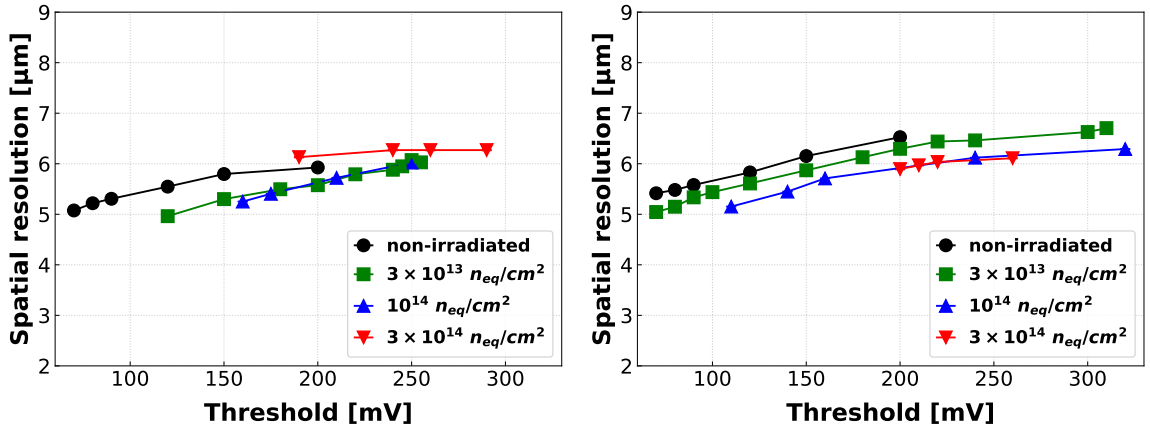

(a) "n-gap" DC-pixels.

(b) "n-gap" AC-pixels.

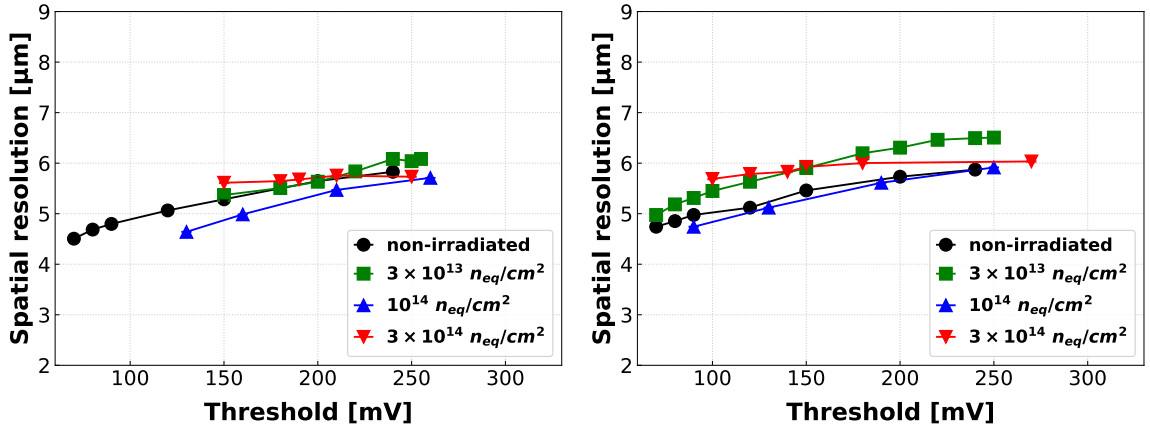

(c) "p-stop" DC-pixels.

(d) "p-stop" AC-pixels.

Figure 7. Spatial resolution as function of the threshold of the "n-gap" DC- (a) and AC-pixels (b), and "p-stop" DC- (c) and AC-pixels (d). The different irradiation levels are shown in different colors.

ionizing radiation dose is concluded in figure 8. It shows the detection efficiency and fake hit rate for the AC-pixels of the three pixel types, after a combined irradiation dose (~5 MRad TID and ~10^{14} n_{eq}/cm^2 NIEL fluences), as function of the threshold (left plot) or High-Voltage (right plot). The left plot shows an excellent detection efficiency for the three pixel types, with a mild drop in that of the "standard" pixel at high thresholds. It was expected, but yet not proven, that the additional HV will improve the charge collection, which will result in better detection efficiency. In the right plot we show the performance achieved with a HV scan from 7 V to 20 V, for the three pixel types. A noticeable improvement in detection efficiency (in blue), as we increase the HV, is observed for the "standard" process (solid line), allowing to reach values of ~99% at 20 V. For the other types, the initial performance allows only for a marginal improvement. The fake hit rate in both plots stays in an acceptable range below 10^{-5}, knowing that an improvement of two orders of magnitude can be achieved when masking a maximum of 10 pixels out of the whole pixel matrix.

2025 JINST 20 C08009

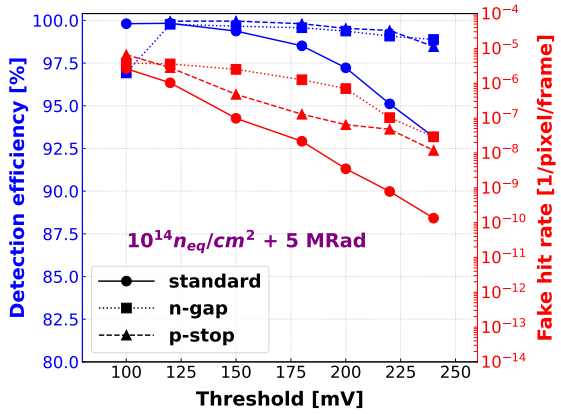

(a) Detection efficiency and fake hit rate as function of the threshold of AC-pixels for combined-irradiated chips.

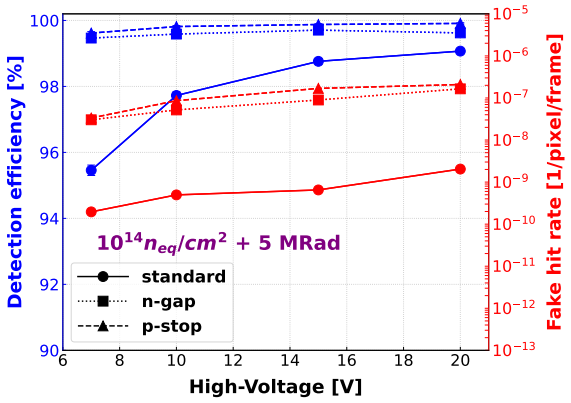

(b) Detection efficiency and fake hit rate as function of the applied HV of AC-pixels for combined-irradiated chips at 200 mV threshold and -1 V BB.

Figure 8. Detection efficiency and fake hit rate for the 3 pixel options after a combined-irradiated dose (~5 MRad TID and ~10^{14} n_{eq}/cm^2 NIEL fluences).

5 Summary, conclusion and outlook

The performance of the MIMOSIS-1 sensor designed for the CBM-MVD was evaluated in beam tests done at DESY and CERN. In this work we reported on the sensor performance after being irradiated to different NIEL fluences of up to ~3×10^{14} n_{eq}/cm^2, accompanied by other results after an additional TID with X-rays. The radiation hardness capability was evaluated based on the desired detection efficiency, fake hit rate and spatial resolution. The results for the two radiation-optimized pixel options (and whether DC or AC), of this first full-size prototype, showed that the sensor achieved a performance level of ~5 MRad TID and ~10^{14} n_{eq}/cm^2 NIEL fluences, complying with the MVD requirements. The standard pixel showed a limited performance that can be improved by selecting low thresholds or applying the highest possible High-Voltage (20 V) for the AC-pixels. Tests for higher fluences showed a limited performance. Apart from the "standard" pixel, for the rest pixel options no noticeable privilege of one type over the other was observed, whether it was while comparing "n-gap" to "p-stop", or DC-pixels to AC ones. This left uncertainties on which pixel option to decide for the consecutive sensor prototype, MIMOSIS-2, which was fabricated already with the three epitaxial layer types, and hosting both DC and AC pixels. The final decision on the pixel type of MIMOSIS-3 will be done based on the results of the ongoing tests of MIMOSIS-2, which will be reported in future works.

Acknowledgments

The measurements leading to these results have been performed at the Test Beam Facility of DESY Hamburg (Germany), a member of the Helmholtz Association (HGF). The authors wish to thank the DESY test beam team as much as Alexander Dierlamm and coworkers from KIT for their help in irradiating the sensors. This work has been funded and supported by the German federal Ministry of Education and Research (BMBF), the European network for developing new horizons for RIs (Eurizon) and HGS-HIRe for FAIR.

2025 JINST 20 C08009

References

[1] J. Stroth et al, *Technical Design Report for the CBM: Micro Vertex Detector (MVD)*, GSI-2022-00549 (2022), https://edms.cern.ch/ui/file/2738980/LATEST/MVD_TDR*.pdf.

[2] CBM collaboration, *Challenges in QCD matter physics –The scientific programme of the Compressed Baryonic Matter experiment at FAIR*, *Eur. Phys. J. A* **53** (2017) 60 [arXiv:1607.01487].

[3] B. Arnoldi-Meadows et al., *Results from single event effect tests with MIMOSIS-1*, 2023 *JINST* **18** C04002.

[4] H. Darwish et al., *Response of the MIMOSIS-1 CMOS Monolithic Active Pixel Sensor to particle beams with different dE/dx*, *Nucl. Instrum. Meth. A* **1062** (2024) 169201.

[5] H. Darwish et al., *Tolerance of the MIMOSIS-1 CMOS Monolithic Active Pixel Sensor to ionizing radiation*, 2023 *JINST* **18** C06013.

[6] ALICE collaboration, *ALPIDE, the Monolithic Active Pixel Sensor for the ALICE ITS upgrade*, *Nucl. Instrum. Meth. A* **824** (2016) 434.

[7] W. Snoeys et al., *A process modification for CMOS monolithic active pixel sensors for enhanced depletion, timing performance and radiation tolerance*, *Nucl. Instrum. Meth. A* **871** (2017) 90.

[8] ATLAS collaboration, *MALTA: a Monolithic Active Pixel Sensor for tracking in ATLAS*, 2020 *JINST* **15** C03019.

[9] IPHC-PICSEL group, *TAF analysis framework*, https://github.com/jeromebaudot/taf.

[10] M. Deveaux et al., *Observations on MIMOSIS-0, the first dedicated CPS prototype for the CBM MVD*, *Nucl. Instrum. Meth. A* **958** (2020) 162653 [arXiv:1909.05614].

[11] M. Mager, *The Telescope Optimizer*, https://mmager.web.cern.ch/telescope/tracking.html.

2025 JINST 20 C08009